# C-H bonds in Carbon Nanotubes as an Energy Carrier

## Investigators

Principal Investigators: Anders Nilsson (SSRL), Bruce Clemens (Materials Science and Engineering), Hongjie Dai (Chemistry)
Hirohito Ogasawara (staff scientist, SSRL), Daniel Friebel (postdoc, SSRL), Srivats Rajasekaran (PhD student, Materials Science and Engineering), Xiaolin Li (postdoc, Chemistry), Ranadeep Bhowmick (PhD student, Materials Science and Engineering), Cara Beasley (PhD student, Materials Science and Engineering)

## Abstract

We investigate the capability of single-walled carbon nanotubes (SWNT) as a possible material for hydrogen storage through the reversible formation of stable C-H bonds using electrochemical means. We have previously shown that the exposure of SWNTs to a source of atomic hydrogen leads to successful hydrogenation without degradation of the nanotube material. We are now investigating alternative hydrogenation reaction pathways that require significantly lower activation energy. The overall hypothesis is to observe if hydrogenation can be induced electrochemically. We reported last year that indeed we observe a current in the I-V curve that could indicate electrochemical storage but other interpretation is also possible. We have therefore undertaken a major effort to establish if there exists a spill-over mechanism where hydrogen becomes adsorbed on Pt catalyst surface which can diffuse to the nanotubes in a second step to form strong C-H bonds. We found that SWNTs can be hydrogenated by exposure to molecular hydrogen if they are modified with a Pd or Pt nanoparticle catalyst. Using x-ray photoelectron spectroscopy we found direct evidence for this "spillover" mechanism. The electrical conductivity of the nanotubes doped with Pt nanoparticles was also measured as a function of exposure to hydrogen gas. The conductivity of the nanotubes decreases with increasing hydrogen exposure. A detailed analysis of the conductivity decrease allows us to model the kinetics of the hydrogenation reaction. In order to prepare non bundled nanotubes we have undertaken a major effort to separate individual tubes. The results indicate that this indeed can be carried out with great success.

### Sample growth/preparation (Clemens group)

The as grown CVD mat samples used in both the XPS measurements and the conductivity measurements were grown in an atmospheric CVD system utilizing isopropanol as the carbon source. The growth temperature was varied from 700°C to 800°C in order to change the density of SWNTs in the mat and the overall mat thickness. The gas flow rates were also used to influence the density and thickness of the mats produced. All of the samples were grown on ~2Å thick film of cobalt metal deposited on silicon oxide wafers with ~50 nm of oxide. The growth conditions can be used to modify the ratio of semiconducting SWNTs to metallic SWNTs in the future to study whether or not SWNT type and diameter impact hydrogen storage

### XPS studies of Nanotube hydrogenation (Nilsson group)

We used x-ray photoelectron spectroscopy (XPS) performed at SSRL beamline 13-2, elliptical undulator beam line, to study the effect of high pressure treatment of Pt-modified carbon nanotubes with molecular hydrogen using a Scienta R5000 detector. Two types of samples were used to test the possibility of hydrogen "spillover" to form C-H bonds.

1) The Dai group deposited thin Langmuir-Blodgett (LB) film of nanotubes onto a native oxide covered Si substrate.
2) Horizontal mats of carbon nanotubes were directly grown on native oxide covered Si substrates using 2 Å cobalt as the catalyst for nanotube formation. These as-grown films were prepared by

the Clemens group. The horizontal mats did not show any contribution of Co in the XPS which indicates that these are thicker samples.

Pt nanoparticles were then sputtered onto these samples. The XPS of the samples before and after hydrogen exposure was measured. The strongest component at 284.8 eV binding energy is assigned to $sp^2$-hybridized C atoms in the nanotubes.

After exposure to hydrogen at a pressure of 120 psi, we observe a significant shoulder at 285.6 eV binding energy (Fig. 1 and 2). The figures below show the XPS before and after hydrogenation for LB films which were sputtered with 6 Å Pt nanoparticles. These plots were normalized with respect to peak height to enhance the changes in the features. This new contribution is assigned to the rehybridization of C atoms to $sp^3$ due to the breaking of $\pi$-bonds and C–H bond formation and can be seen as a direct evidence for the proposed spillover effect.

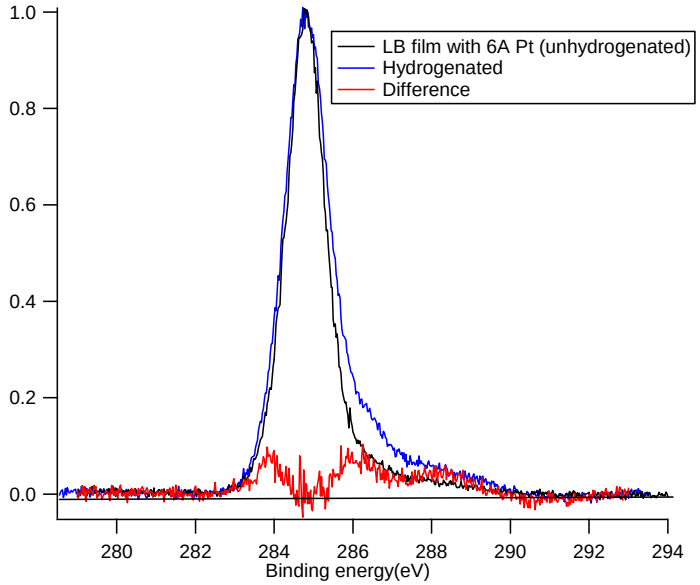


**Fig. 1:** XPS before and after hydrogenation of LB films

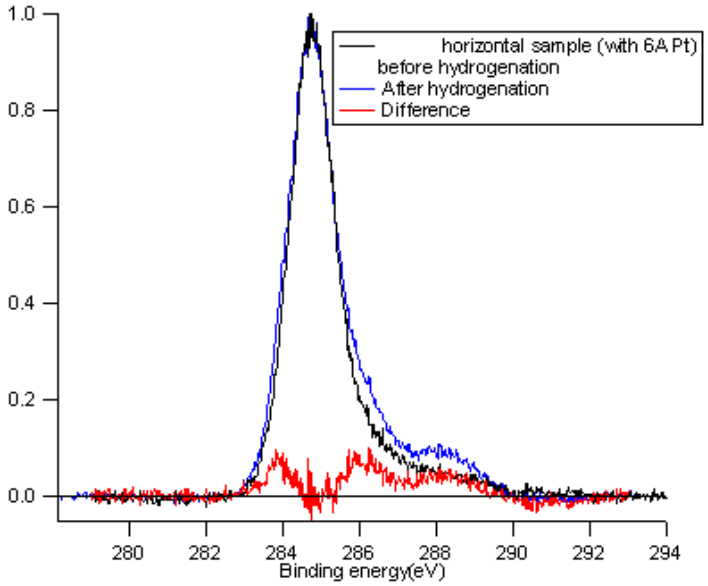


**Fig. 2:** XPS before and after hydrogenation of As-grown films

Furthermore, an additional new peak at 288eV can be detected for both hydrogenated samples. We conjecture that this peak arises from a metal-to-semiconductor transition of the nanotubes that is induced by the hydrogenation. The accompanying decrease of the electric conductivity can cause a reduction of the core hole screening, resulting in a ~4 eV higher final state energy. Alternatively, the creation of a band gap can give rise to a shake-up line.

By deconvoluting the XP spectra as shown in Figure 3, we can estimate the amount of carbon atoms that has undergone a change from $sp^2$ to $sp^3$ hybridization, which corresponds to the amount of stored hydrogen. The relative weights of the $sp^2$ ($sp^3$) peaks are 0.84 (0.17) for the LB film and 0.87 (0.13) for the as-grown film. The third peak at 288eV has a relative weight of ~0.05 in both samples. Since the fraction of hydrogenated carbon atoms is proportional to the relative peak intensity, we obtain atomic hydrogen percentages of 16% for the LB film and 12% for the as-grown film. If all carbon atoms were hydrogenated, the hydrogenation would be 7.7 weight percent. Therefore in this experiment the weight percentage hydrogen uptake is 1.2% for LB films and 1 % for the as-grown films.

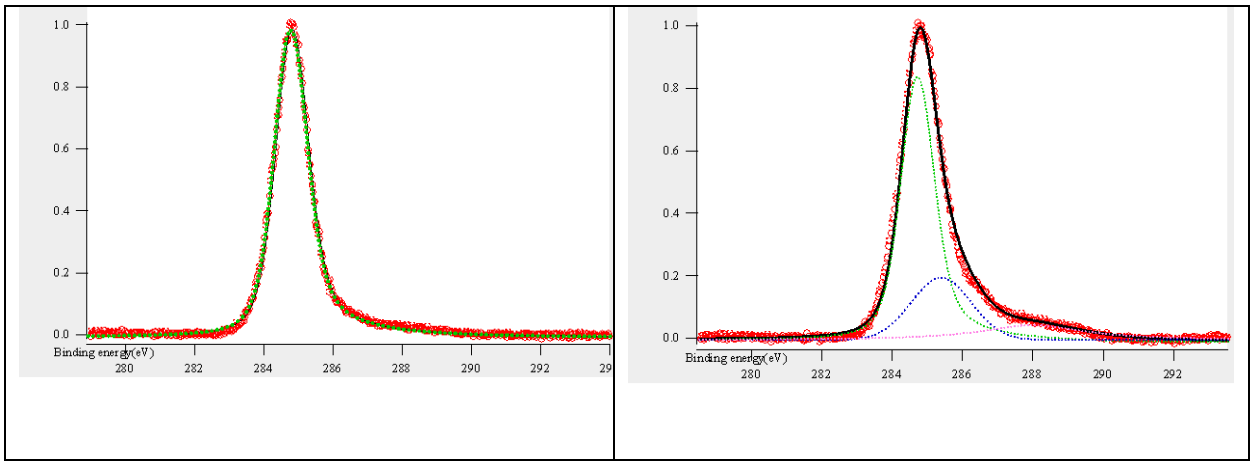


**Fig. 3:** Fitted XPS peaks of LB films, before (left); and after Hydrogen exposure (right)

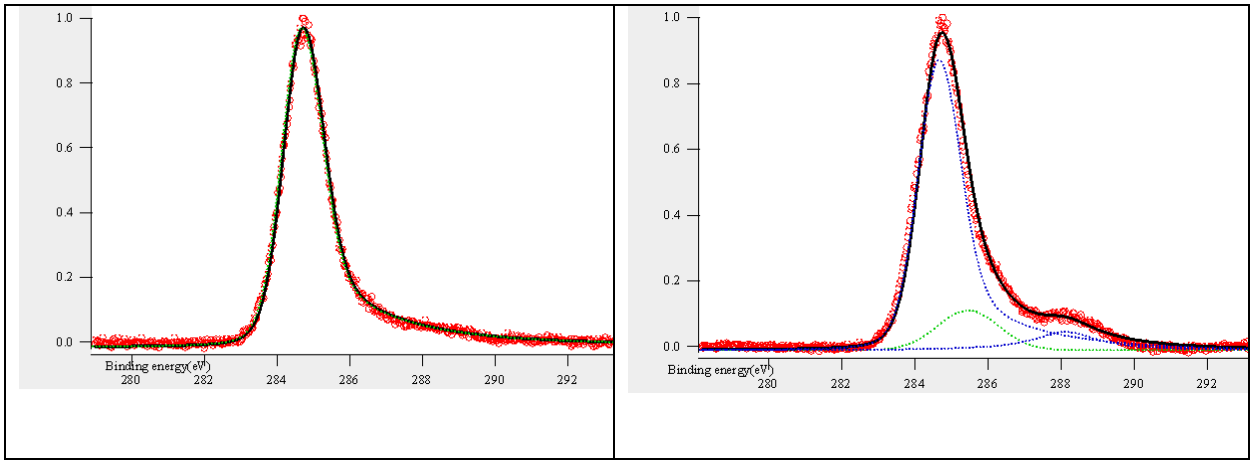


**Fig. 4:** Fitted XPS peaks of as-grown samples, before (left); and after Hydrogen exposure(right)

This leads us to the conclusion that the exposure of Pt-modified CNTs to molecular hydrogen results in the successful formation of stable C-H bonds. Our results demonstrate that the hydrogenation mechanism is a spillover process where hydrogen molecules first dissociatively adsorb on the Pt surface, and the chemisorbed H atoms subsequently diffuse ("spill over") onto the nanotube surface where they can form C-H bonds. Our previous findings which we reported in 2008 are not only confirmed by the new results but, moreover, due to improvements in the preparation of our Pt-modified CNT samples we were

able to achieve a higher yield of C–H bonds whose spectral features, due to higher purity of the samples, could be more clearly detected.

We also explored the possibility of hydrogen storage in other forms of nanotubes, e.g. as-grown films of vertically aligned nanotubes. Pt nanoparticles were sputtered on the samples and tend to reside on top of these films. The nanotubes show a broad XPS peak width, indicating the presence of many defects in the nanotube structure such as $sp^3$-hybridized or oxygenated carbon species. This can be explained since XPS, which is a surface sensitive technique, mostly probes the upper ends of the nanotubes which are known to be rich in defects. Exposure of these samples to hydrogen under a pressure of 120psi does not seem to cause significant changes in the shape of the C 1s signal, whose overall intensity, however, appears to have decreased after the hydrogen treatment. The latter could be explained with a higher reactivity at the defect sites where atomic hydrogen generated on the adjacent Pt particles etches the nanotube, resulting in the removal of carbon (e.g., as $CH_4$) rather than the non-destructive addition of hydrogen to a stable nanotube structure.

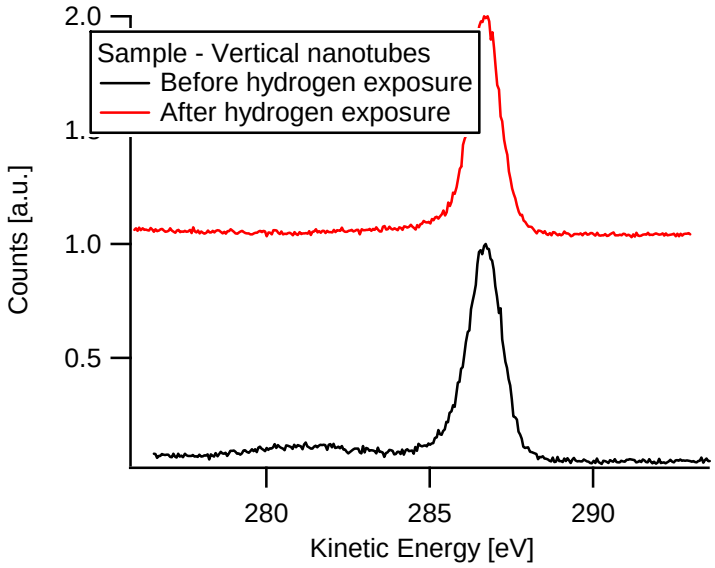


**Fig. 6:** XPS of vertical nanotubes before and after hydrogen exposure

Vertically aligned nanotubes, sputtered with 5 Å Pt, were also used to further explore a possible electrochemical pathway for hydrogen storage. First, the sample was immersed into an electrolyte solution of 0.01 M $H_2SO_4$ without applying an electrochemical potential; after this treatment we already observed a significant broadening of the C 1s region in the XPS. This broadening is certainly not related with hydrogenation but can be caused either by adsorption of an organic impurity from the electrolyte, or, since traces of oxygen are present in the electrochemical cell, a spontaneous oxidation resulting in carbon-oxygen bonds or a higher amount of defects in the nanotubes. In a subsequent experiment, the sample was immersed again and a potential of -1.0V was applied for 10min, the reference electrode being Ag-AgCl standard electrode. After this second treatment in the electrolyte, we measured a C 1s signal whose width is in between those found before and after the first immersion experiment. Hence, the amount of impurities that had been introduced by the immersion without potential control decreased due to the treatment at -1.0 V, either by decomposing previously adsorbed organic impurities or by removing defective nanotube material in a mechanism similar to the hydrogen-etching observed under gas-phase hydrogenation conditions. We will in the near future investigate if electrochemical hydrogenation is feasible using the LB films where we clearly could observe the splill-over mechanism with gaseous loadings as described above.

## Four-probe conductivity Tests (Clemens group)

## Motivation

An uptake in hydrogen enhancement of transition metal doped SWNT has been reported [1-3]. The reason for this enhanced uptake has been attributed to the aptly named "spillover effect" mechanism. Molecular hydrogen is dissociated by a metal catalyst diffuses to the surface of nanotubes (spills over), where it forms stronger bonds with the nanotube surface. However, a healthy amount of speculation exists about the validity of the spillover mechanism. The amount of hydrogen uptake by passing molecular hydrogen on catalyst doped SWNT is <1wt%, in addition to it having very slow kinetics. Therefore there is need to further investigate the spillover process. Hence, in-situ 4-probe tests were performed to study the change in conductivity of the doped SWNT film during the hydrogen charging. A 4-probe test is needed because it eliminates the contact resistance between the probes and the material, and hence any change in resistance of the sample is solely due to the change in resistance of the material. A constant current was passed through the outer probes and the potential difference in between the two inner probes was monitored as a function of charging time.

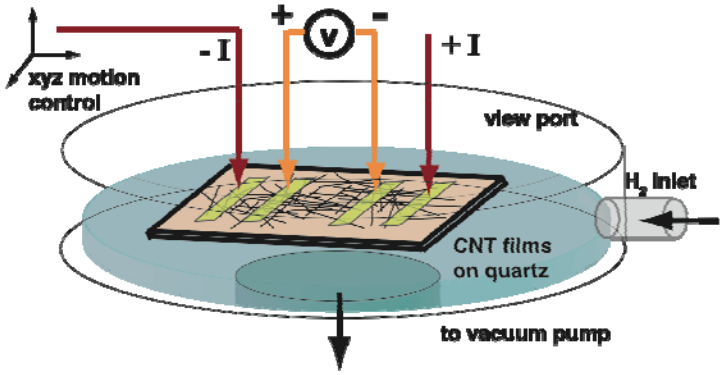


**Fig. 7:** Four-probe setup for conductivity measurements on CNT samples

Fig. 7 is a schematic of the 4-probe set-up used for this study. The chamber can be evacuated using a turbo pump backed by a roughing pump. All the four probes have xyz motion controls, and an optical microscope connected to a CCD camera is used to ensure electrical contact with the material. The only disadvantage is that the view port is not rated for positive pressures and hence the effect of hydrogen pressure above an atmosphere cannot be studied. To increase the signal to noise ratio the 4 probes are connected to an Agilent 4156B Semiconductor Parameter Analyzer via biaxial and triaxial cables. Ports on the side can be used for gas flow into the chamber and also for electrical feed-throughs. An embedded heating element is used for temperature dependent hydrogen charging experiments. Metal pads were sputter deposited on the SWNT film to facilitate good electrical contact with the 4 probes.

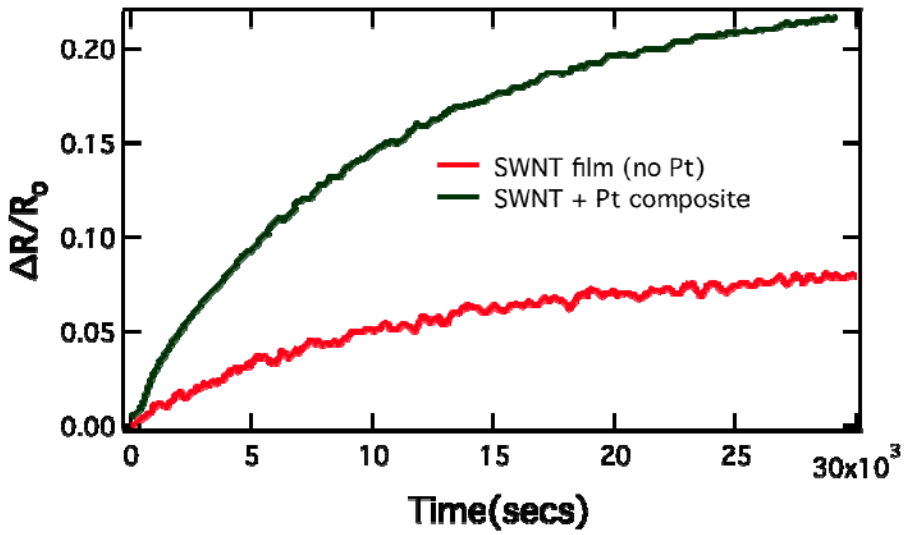


**Fig. 8:** Resistance change as function of hydrogen charging for Pt-free and Pt sputtered CNT samples

Fig. 8 plots the change in resistance as a function of hydrogen charging before and after sputtering Pt on the thin SWNT films. The films were exposed to 760 Torr of hydrogen pressure, after evacuating the chamber down ~mTorr. The change in resistance of the Pt-SWNT composite film is approximately 4 times the resistance change for the un-doped film. The hydrogen enhancement could be attributed to spillover of H atoms from hydrogen molecules that dissociatively chemisorbs on the Pt nano catalyst particle surface. The increase in resistance is also circumstantial evidence of the formation of H bonds on the SWNT surface. This is because Wessely et al. [4] showed that the presence of H induces a substantial component of $sp^3$ bonding as a result of which the $\pi$ and $\pi^*$ components of the electronic structure vanish.

Next we studied the increase in resistance of the films as a function of the nominal thickness of the sputter deposited Pt films. This is shown in Fig. 9.

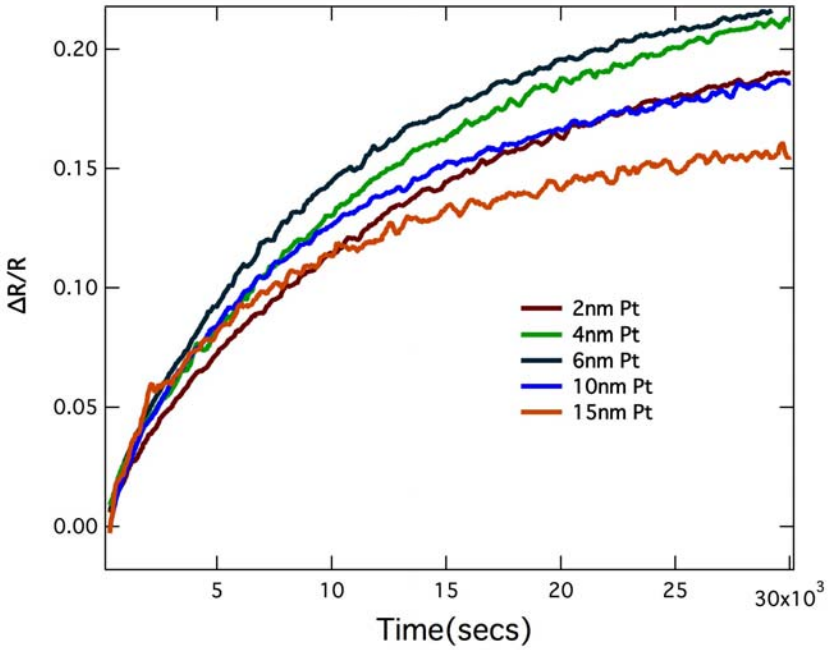


**Fig. 9:** Resistivity changes with hydrogen exposure for CNTs with different Pt loadings

With increase in nominal thickness of the catalyst particles the normalized resistance initially increases till an optimal level, beyond which it decreases. The optimal thickness of the deposited Pt film is 6 nm. It has been observed before that the hydrogen uptake by a Pt-SWNT composite film varies linearly with the density of the Pt particles. With an increase in the nominal thickness of the Pt film, the density as well as the size of the catalyst particles increase. But, beyond a certain thickness of sputtered film, the Pt particles start agglomerating, thus decreasing the number density of the particles and hence decreasing the extent of H spillover onto the SWNT surface.

For the next experimental set, the nominal thickness of the sputtered Pt film was kept constant, but the thickness of the SWNT film was varied. For this study five different SWNT films were used: HiPCO SWNT dispersed in iso-propanol and spin cast on glass, dense and sparse distributions of horizontal SWNT mats grown from Co catalysts on glass, and finally two monolayer thick SWNT films of varying densities assembled by the Langmuir Blodgett (LB) method.

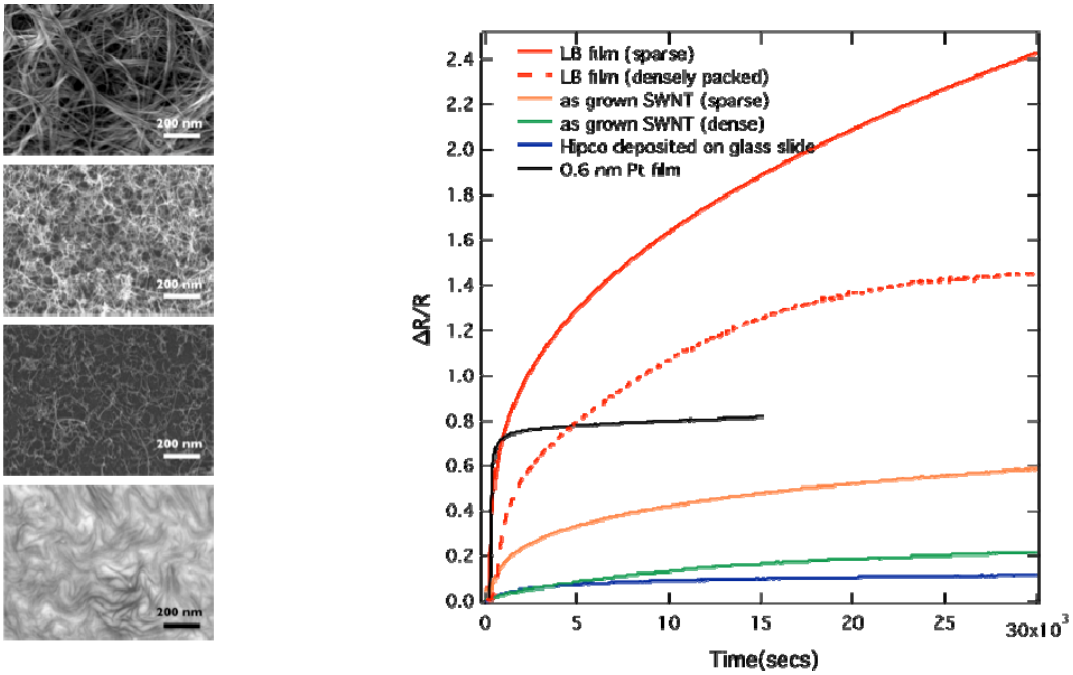


**Fig. 10:** Hydrogen uptake efficiency for SWNT films with varying thickness. The Pt loading was kept identical for all samples.

Hydrogen uptake by the Pt-SWNT composites has a strong dependence on the thickness of the SWNT mats; the sparse SWNT LB films show an increment of more than an order of magnitude in resistance values compared to the HiPCO SWNT films spun cast on glass. This dependence is attributed to the numerical density of Pt particles per area of the SWNT film exposed to hydrogenation, which is the least for the thick HiPCO films and highest for the LB films. Thus for maximum hydrogen storage it is necessary to obtain a uniform dispersion of monolayer thick unbundled SWNTs, doped with optimal size and density of Pt catalyst particles. This would ensure a high specific hydrogen uptake per weight of Pt-SWNT composite. Of, special note is the solid black line in the Fig. 10, which plots the resistance change of a bare 0.6 nm Pt thin film exposed to hydrogen. Similar to the SWNT-Pt composite films, the resistance of the Pt film increases probably due to the change in Fermi level of Pt on exposure to hydrogen. But, the time scale for the change in resistance of the Pt film is much smaller than the SWNT-Pt composites implying that the change in resistance of the composites cannot be attributed to surface-hydride formation of the Pt nanoparticles. This provides indirect evidence for the validation of the spillover process.

The time for all the hydrogenation experiments mentioned so far is approximately 8 hours. It was observed that even after 8 hours the resistance plots do not reach a plateau region, implying very slow kinetics. If the hydrogen uptake is via the spill over mechanism, then the kinetics could be limited by the diffusion of C over the SWNT surface. In that case, the temperature of the charging process would

influence the kinetics and possibly result in an uptake increment with temperature. Fig. 11 plots the temperature dependence of resistance change for a film on exposure to 760 Torr of hydrogen.

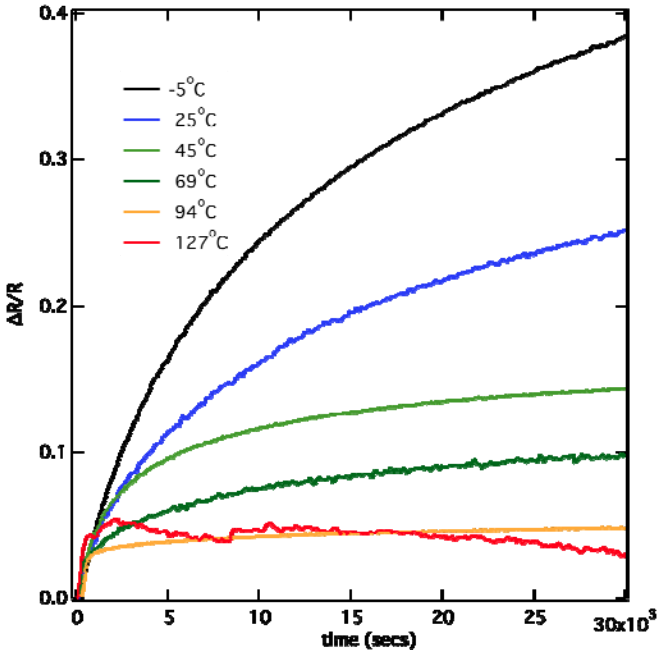


**Fig. 11:** Hydrogen uptake measured at different temperatures

It is observed that the rate of change in resistance increased on ramping up the hydrogenation temperature from -5°C to 127°C. This again provides indirect evidence for the spillover process. But, interestingly the net change in resistance of the films decreased on ramping up the temperature. The net change in resistance and hence the amount of hydrogen uptake is largest for -5°C and kept on decreasing monotonically on increasing the hydrogenation temperature. This behavior can be attributed to the exothermic nature of the hydrogen dissociation reaction on Pt. Increasing the temperature would decrease the Pt- surface hydride formation [5] and hence the amount of H spillover onto the SWNT surface. The above sets of experiments also show that 4-probe studies can be used as a very simple, sensitive probe to optimize the hydrogen uptake conditions for doped SWNT films.

## Separation of individual single-Walled Carbon Nanotubes from Bindled Nanotubes (Dai group)

Single-walled carbon nanotubes (SWNTs) are a unique class of macromolecule, conceptualized as a single graphitic sheet of $sp^2$ carbon atoms, rolled into a seamless cylinder, with diameters of ~ 0.5 – 1.6 nm, and lengths from tens of nanometers up to millimeters. For various applications of nanotubes, it is necessary to obtain individual SWNTs rather than bundled nanotubes, to maximize the surface area for applications such as hydrogen storage and optimize the physical properties of nanotubes such as photoluminescence and resonance raman scattering.

Unfortunately, as-grown SWNTs are heavily bundled. The Dai group set out to obtain purely individual SWNT samples desired for hydrogen storage. We used density gradient centrifugation (DGC) rate (zonal) separation for sodium-cholate suspended SWNTs through an iodixanol step-gradient at ~300,000 g. This method separates nanotubes by mass, with fractions rich in single tubes floating on top of the column and bundles settling at the lower parts of the centrifuge column, as shown in Fig.12. We used fluorescence, Raman and UV vis spectroscopy to characterize the individual and bundled fractions of SWNTs, described below.

Resonance Raman scattering analysis, under 785 nm laser excitation, of the DGC separated SWNT fractions showed similar intensity trends as the relative PL measurements (Fig.13), for both the

radial breathing modes (RBMs) and graphitic band (G-band). The DGC separated and absorbance-normalized fractions of SWNTs showed a sharp rise in Raman scattering intensity from fractions 3-6, with a peak in both the RBM and G-band scattering intensity in fraction 6, coinciding with the peak in PL QY. This peak is followed by a gradual decrease in intensity for both modes (Fig.13a,b). Similar trends were observed for Raman scattering spectra measured at 633 nm excitation.

The cause of the gradual loss of both PL QY and Raman scattering intensity in higher fractions is due to presence of small nanotube bundles. Bundling of dispersed SWNTs is known to reduce PL QY via non-radiative energy transfer processes. Excitons can decay non-radiatively into a neighboring metallic nanotube, leading to quenching of the photoluminescence. Bundling also causes red-shifting and absorption peak broadening of the excitonic optical transitions in SWNTs. We observed a red-shift of 13 nm (25 meV) for the optical transition near 800 nm (Fig. 13c and 14a) with increasing fraction number. Broadening of optical transition peaks was also observed, suggesting the presence of a broad distribution in the degree of SWNT bundling. Indeed, Raman scattering analysis revealed an increase in (10,2) RBM intensity indicating an increase in SWNT bundling following DGC, in fraction 7 and above (Fig.14b). This phenomenon results from increased resonance-enhancement of the radial breathing mode of the (10,2) SWNT at 785 nm excitation, caused by the red-shifting of optical transitions associated with bundling.

The decrease in Raman scattering intensity in higher fractions is related to the red-shifting of the SWNT optical transitions, following from an increasing proportion of SWNT bundles with increasing fraction number. Bundling of SWNTs, perturbs the SWNT single-particle band structure and increases dielectric screening effects, which in turn reduce excitonic optical transitions. This effect is in part mitigated by a decrease in exciton binding energies, but overall the band structure effects outweigh excitonic effects. Charge transfer, caused either by interactions of SWNT sidewalls or the π-density contribution of small aromatic molecules, leads to increased coulomb interactions, and subsequent carrier charge screening, that reduces exciton lifetimes, and leads to PL quenching and contributes to the broadening of optical transitions.

In summary, we have performed density gradient centrifugation (DGC) of sodium cholate-suspended SWNTs in water to separate individual nanotubes from small bundles. Long, individual SWNTs are obtained based on spectroscopy measurements. Our method obtains fractions of highly individualized nanotubes, which are now available for hydrogen storage experiments. However, a major next hurdle is to scale up such individual SWNTs to large quantities needed for future realistic storage applications.

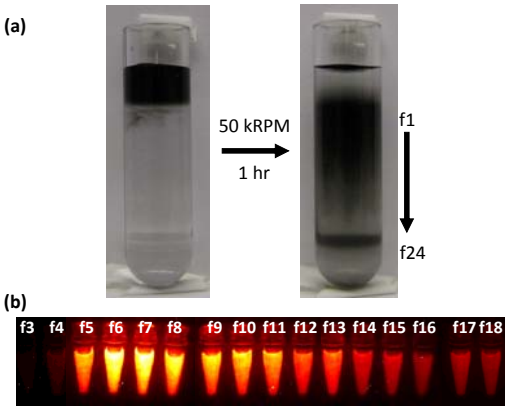


**Fig. 12:** Centrifugation of sodium cholate-suspended single-walled carbon nanotubes (SWNTs) through a density gradient containing 1% sodium cholate, with discontinuous steps of 5%/10%/15%/20%/60% iodixanol at 50,000 RPM for one hour yielded a continuous distribution of SWNTs as well as a band formed at the 60% iodixanol boundary, as is clear from **(a)** photographs taken before and after DGC. (b) photoluminescence under 808 nm excitation showed varying relative quantum yield which is a measure of individual SWNT concentration, increasing from f3 to f6-7 and decreasing monotonically thereafter. F5-f8 are fractions highly enriched in individual SWNTs.

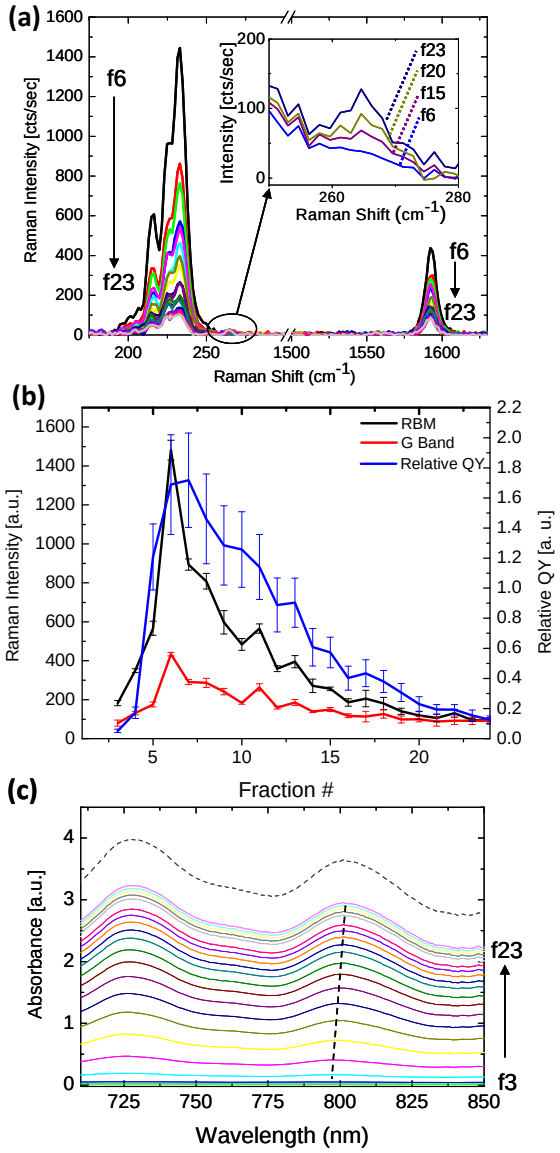


**Fig. 13:** Spectroscopy characterizations of separated SWNT fractions. Individual SWNTs show much higher fluorescence and Resonance raman than bundled fractions. **(a)** 785 nm excitation Raman scattering spectra of DGC separated SWNTs at the same OD. Greater sensitivity is observed for the RBM peaks compared with the G-band peak, yet both features follow the same monotonic decrease in scattering intensity from f6-f23. An increase in intensity is observed for the RBM at 266 $cm^{-1}$ corresponding to the (10,2) chirality (inset) with increasing fraction number. **(b)** Comparison of Raman scattering for the RBM at 233 $cm^{-1}$ and G-band at 1590 $cm^{-1}$ on the left axis with relative quantum yield, on the right axis, versus increasing fraction number. All three spectral features show an initial increase in intensity followed by a decrease. **(c)** Near-infrared absorbance spectra for the DGC separated SWNT fractions shown in **(a)** as well as the cholate-SWNT starting material (dotted line). Red-shifting of the optical transition peaks was observed monotonically with increasing fraction number (curves are offset for clarity).

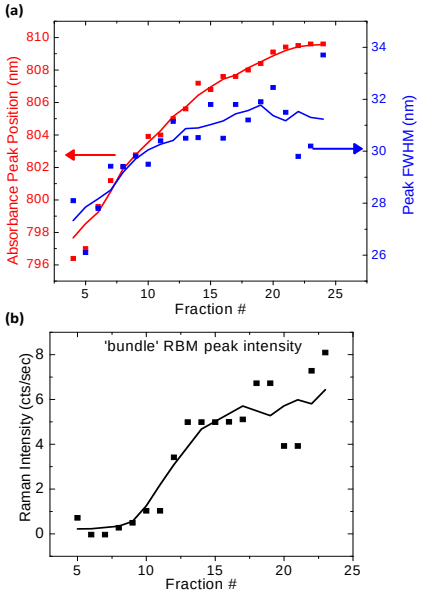


**Fig. 14:** Spectral properties of the SWNT optical transition near 800 nm. **(a)** Absorbance peak position and full-width at half-maximum tend to increase with increasing fraction number. The arrows indicate the absorbance peak position and FWHM, respectively, of the cholate-SWNT starting material, before DGC separation. **(b)** Peak intensity for the SWNT RBM feature at 266 $cm^{-1}$, referred to as the "bundle peak," following 785 nm excitation, with increasing fraction number.

## References


(1) Lueking A.D. et al. Hydrogen spillover to enhance hydrogen storage study of carbon physicochemical properties. - *Appl. Catal.A.* **2004**, *254,259.*

(2) Kokabas S. et al. Effect of thermal treatments and palladium loading on hydrogen sorption characteristics of SWNT. *Intl. Jl. Of Hydrogen storage.* **2008**, *33*, 1693.

(3) Lee Y.W. et al. Novel Sievert's type volumetric measurements on hydrogen storage properties for very small quantities. *Jl. Alloys and Compds*. **2008,** 452,410.

(4) Wessely O. et al. Dynamical core-hole screening in the x-ray absorption spectra of hydrogenated carbon nanotubes and graphene. *Physical Review B.* **2007**, 76,161402-1.

(5) Legare P. A theoretical study of H surface and subsurface species on Pt (111). *Surface Science.* **2004,** 559,169.